

Dependence of the surface resistance of niobium coated copper cavities on the coating temperature.

P. Darriulat, C. Durand, P. Janot, N. Rensing and W. Weingarten, CERN and P. Bosland, J. Gobin and J. Martignac, C.E. Saclay.

Abstract

Six hydroformed copper 1.5 GHz cavities have been baked and coated with niobium at different temperatures between 100 °C and 200 °C, while keeping the other discharge parameters unchanged. Their surface resistance has been measured as a function of RF field and trapped magnetic field. Its dependence on deposition temperature confirms earlier indications obtained using 350 MHz LEP cavities that 150 °C leads to optimal performances. The critical temperatures of Nb/Cu and bulk Niobium cavities have also been measured : the result obtained for Nb/Cu, $9.56 \text{ K} \pm 0.02\text{K}$, differs from the Nb value, $9.231 \text{ K} \pm 0.007\text{K}$, in qualitative agreement with expectation from the different lattice parameters.

different temperatures, all other parameters being kept unchanged. The dependence of their quality factor Q on accelerating gradient E , on temperature T , and on a possible external magnetic field H_{ext} , applied when cooling down the cavity below the critical temperature T_c , has been studied. The results are parametrized in a simple ad hoc form, inspired from theoretical expectations, and allowing for straightforward comparisons in terms of only a few parameters. These include a residual, T independent, surface resistance R_0 measured at $E = H_{\text{ext}} = 0$ in excess of the T dependent BCS resistance and an effective slope parameter σ describing the non quadratic losses to first order.

We also report on a comparative measurement of the critical temperature for niobium copper and bulk niobium cavities respectively.

1. Introduction

Niobium copper cavities (i.e. copper cavities internally coated with a thin superconducting niobium layer) have been developed for the LEP energy upgrade project [1]. As reported in these Proceedings [2], they are currently being produced by industry and routinely meet their design specifications (a quality factor Q of $4 \cdot 10^9$ for an accelerating gradient $E = 6 \text{ MV/m}$ at a temperature of 4.2K). RF power losses in the cavity walls are an essential factor in the limitation of their performance. At 4.2 K and low accelerating gradient, such losses exceed only slightly the lower achievable value predicted by the BCS theory but they increase with accelerating gradient faster than the predicted E^2 law, resulting in the deterioration of Q by a factor of typically 2 between 0 and 6 MV/m [1]. In an attempt to improve our understanding of the physical processes causing such losses, in particular non quadratic losses (NQL), systematic studies are being performed on 1.5 GHz cavities, easier to handle than the much larger 352 MHz LEP cavities.

We report here on a measurement of the dependence of RF losses on the coating temperature. A set of 6 cavities have been coated at

2. RF Losses

2.1 Cavity production

A set of six monocell 1.5 GHz copper cavities have been coated at Saclay with a 3 μm thick niobium layer using the standard sputtering techniques [3,4]. The main coating parameters were set at constant values: the discharge current at 1.5 A, the cathode voltage at $-380 \pm 10 \text{ V}$ and the Argon pressure at 6.5 μbar , while the temperature of the copper substrate was set at different values ranging between 100 °C and 200 °C as listed in Table 1. The copper temperature was kept constant to within $\pm 4 \text{ °C}$ during the coating operation. The last digit in the labels identifying the cavities (first line of Table 1) indicates the number of successive coatings (separated by a chemical etching) made on the cavity. As previous experience [5] has established that the first coating usually yields poorer performance than successive coatings, cavity C3.1 is considered separately. Cavity A2.3*, which was measured a second time after a high pressure water rinsing, is also considered separately. A bulk niobium cavity, labeled L13, has been used as a reference.

cavity	T coat. (°C)	R _{BCS} (4.2)	R ₀	R _{4.2} ¹	R _{1.7} ¹	σ
L13		694 ± 7	18 ± 2	113 ± 5	4 ± 1	0.124 ± .014
C2.2	100	400 ± 15	75 ± 5	415 ± 10	142 ± 5	0.808 ± .015
A2.3	150	480 ± 15	4 ± 3	176 ± 9	19 ± 2	0.224 ± .034
A2.3*	-	480 ± 15	22 ± 3	176 ± 9	107 ± 8	0.445 ± .015
B4.2	125	443 ± 20	35 ± 4	398 ± 10	165 ± 15	0.856 ± .020
C1.2	175	472 ± 4	6 ± 2	103 ± 9	28 ± 2	0.181 ± .011
B2.2	200	405 ± 11	32 ± 5	315 ± 13	101 ± 3	0.596 ± .040
C3.1	150	479 ± 4	61 ± 2	180 ± 9	90 ± 3	0.430 ± .017

Table 1

2.2 Quality factor measurement

The quality factor of each cavity has been measured in its fundamental mode as a function of E, T, and H_{ext} using standard RF measurement techniques [6]. The cavity was immersed in a liquid helium cryostat shielded from terrestrial magnetic field. The measured residual field was 3 μT. The helium gas pressure could be lowered from 1000 to approximately 15 mbar allowing for temperatures ranging between 4.2 K and 1.6 K. The temperatures were measured using carbon thermometers isolated from the helium bath and in direct contact with the cavity with a precision of the order of 10 mK.

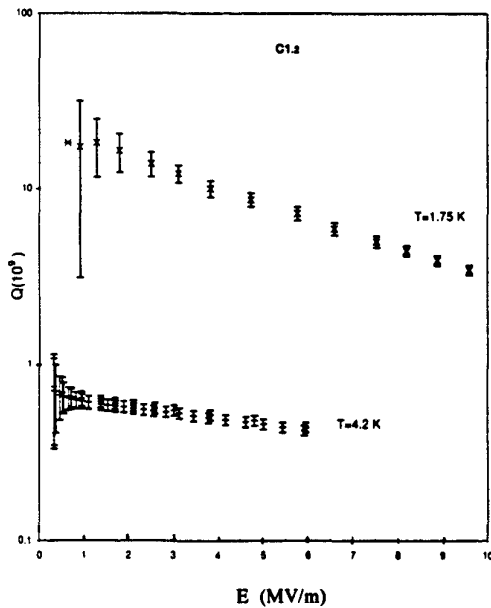


Figure 1.

A uniform external magnetic field ranging between 0 and 10 G, created by a solenoid around the cryostat, could be applied along the cavity axis. In some instances, a non uniform magnetic field created by a pair of Helmholtz coils having their common axis perpendicular to the cavity axis has been applied. In such cases an effective solenoidal field, defined as the solenoidal field causing identical RF losses, will be quoted. A typical measurement of the quality factor Q as a function of accelerating gradient E is shown in Figure 1. Error bars are dominated by uncertainties on the RF power (incident, reflected and transmitted) measurements, depending on the sensor's sensitivity.

2.3 Data parametrization

The data are parametrized using a form

$$R = \frac{295\Omega}{Q} = R_0 + R_{BCS}(T) + R_E(E, T) + R_H(E, T, H_{ext}) \quad (1)$$

with

$$R_E = 0 \text{ for } E = 0$$

$$R_H = 0 \text{ for } H_{ext} = 0$$

$$R_{BCS}(T) = \frac{\alpha}{T} \exp\left(-\frac{\Delta_0}{k_B T}\right)$$

The geometry factor $RQ = 295\Omega$ was calculated by solving the Maxwell equations numerically [7,8]. As α and Δ_0/k_B are found to be strongly correlated we fix $\Delta_0/k_B = 19K$, a value in good agreement with the whole data set, and rewrite:

$$R_{BCS}(T) = R_{BCS}(4.2) \cdot \frac{4.2}{T} \exp\left(\frac{19}{4.2} - \frac{19}{T}\right) \quad (2)$$

leaving $R_{BCS}(4.2)$ and R_0 as only adjustable parameters at $E = H_{ext} = 0$.

As most of the temperature dependence is observed to be caused by the BCS term, we find that a linear temperature dependence is adequate for R_E and R_H and write:

$$R_E(E, T) = F_{1.7}(E) + \frac{T-1.7}{4.2-1.7} (F_{4.2}(E) - F_{1.7}(E)) \quad (3)$$

$$R_H(E, T, H_{ext}) = R_H(E, 3, H_{ext}) (1 + \mu(T-3)) \quad (4)$$

Here $F_T(E)$ requires a quadratic dependence on accelerating gradient of the form (see section 2.4):

$$F_T(E) = R_T^1 \frac{E}{6} (1 + \lambda \frac{E-6}{6}) \quad (5)$$

leaving three adjustable parameters $R_{1.7}^1$, $R_{4.2}^1$ and λ to describe the non quadratic losses (note that NQL's are measured by R_T^1 at $E = 6$ MV/m and by $\frac{1}{2} R_T^1 (1 - \frac{\lambda}{2})$ at $E=3$ MV/m).

The parametrization of $R_H(E, 3, H_{ext})$ is considered in section 2.5.

2.4 Results at $H_{ext} = 0$

The results of the fits to the $H_{ext} = 0$ data are listed in Table 1. In all cases the quality of the fits is found satisfactory, with χ^2 values consistent with the numbers of degrees of freedom. Figure 2 summarizes the results obtained at $E = H_{ext} = 0$ with $(R_0, R_{BCS}(4.2))$ coordinates mapped onto the $Q(E = H_{ext} = 0, T = 1.7)$ vs $Q(E = H_{ext} = 0, T = 4.2)$ space. While all niobium copper cavities are observed to have similar BCS terms, the residual surface resistances vary between 4 and 75 n Ω .

The dependence on accelerating gradient is illustrated in Figure 3 where the values of $R_{1.7}^1$ and $R_{4.2}^1$ obtained for each cavity are plotted. Evidence for the adequacy of the quadratic form used in the parametrization of $F_T(E)$ (Relation 5) is given in Figure 4. In an attempt to define for each cavity a single effective slope parameter σ giving an adequate description of the non quadratic losses, we make use of the fact that the data of Figure 3 cluster around the line $\frac{R_{1.7}^1}{180} = \frac{R_{4.2}^1}{500}$ (although displaying a significant spread around it). We define

$$\sigma = \frac{1}{2} \left(\frac{R_{1.7}^1}{180} + \frac{R_{4.2}^1}{500} \right) \quad (6)$$

A clear correlation is observed between the residual surface resistance R_0 and the effective slope parameter σ (Figure 5) suggesting the simultaneous use of these two parameters to obtain a global evaluation of the quality of the coating. Figure 6 shows the dependence of R_0 and σ upon coating temperature indicating the presence of an optimum in the range $T_{coating} = 150$ °C to 175 °C in agreement with earlier estimates [5]. The data obtained with C3.1 (coated for the first time) and A2.3* (after a high pressure water rinsing) cannot be used in drawing

conclusions on the T coating dependence, as it is essential to compare cavities having been identically treated (apart from the value of T coating).

Q (E = 0, T = 1.7)

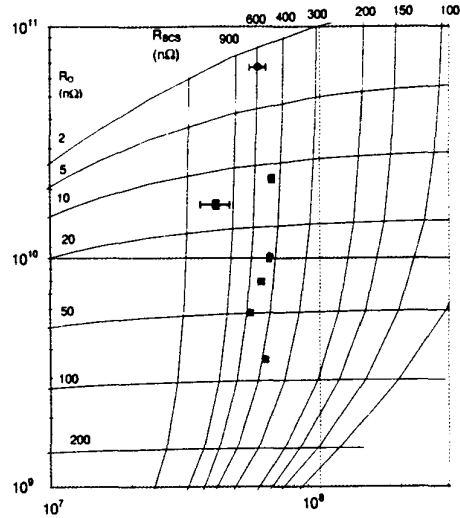


Figure 2. Q (E = 0, T = 4.2)

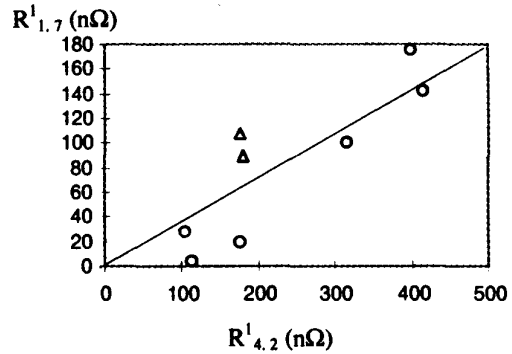


Figure 3.

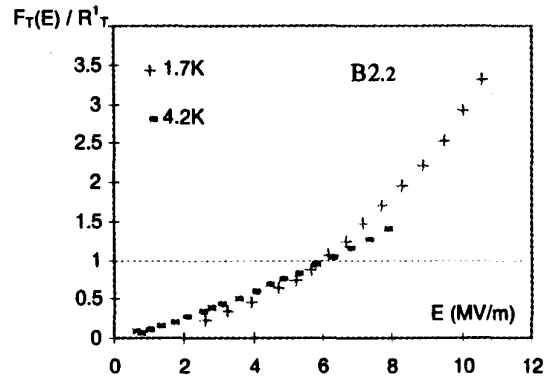


Figure 4.

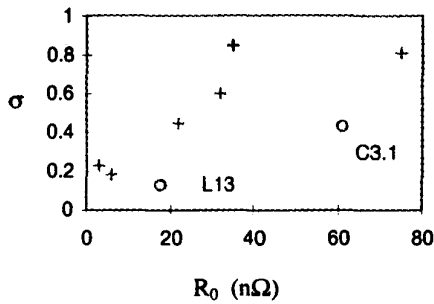


Figure 5.

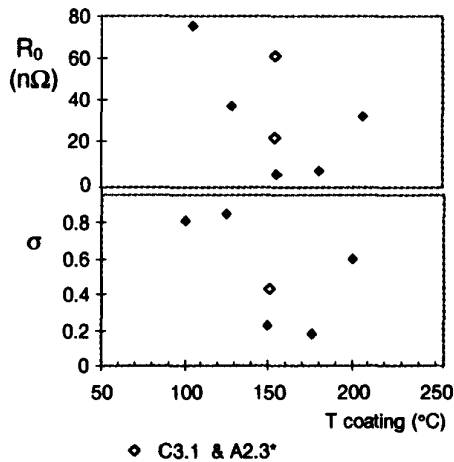


Figure 6.

2.5 Dependence on H_{ext}

The interest of measuring the dependence of RF losses on the intensity of an externally applied magnetic field is twofold. It gives useful information on the sensitivity of the cavity performance in an accelerator environment where extraneous magnetic fields (such as the terrestrial field) are present at the Gauss level and it provides a diagnosis tool to better understand the physics processes at the origin of RF losses. A detailed study of such processes is beyond the scope of the present article. Here we only report on the main qualitative features.

Evidence for complete trapping is obtained by measuring the field distribution outside the superconducting cavity in two different configurations:

- i) the cavity is cooled in the presence of a field generated by the external coils, their current being switched off when its temperature reaches values lower than T_c ,
- ii) the cavity is cooled with no current in the coils, their current being switched on only when its temperature reaches values lower than T_c .

The fields measured in both configurations add up to the field created by the coils when the cavity is in its normal state (transparent magnetic field) and are in good agreement with the solutions of the Maxwell equations assuming complete trapping and complete Meissner expulsion respectively.

These results are in good agreement with earlier measurements [9].

We find that a parametrization of the form:

$$R_H(E, 3, H_{ext}) = H_{ext} (a + b H_{ext} + c E + d E H_{ext})$$

describes adequately the data, leaving four parameters to be adjusted. Figure 7 illustrates the dependence of R_H on E and H_{ext} for the bulk niobium and niobium copper cavities respectively. Here $R_H(E, 3, H_{ext})$ is defined from Relation (1) using the fit results obtained in section 2.4 to describe $R_0 + R_{BCS}(T) + R_E(E, T)$, lines of equal values of R_H being drawn in the E, H_{ext} plane. Qualitative evidence for the adequacy of the above parametrization is observed. The sensitivity of the niobium copper cavities to external magnetic field is seen to be much smaller, by more than one order of magnitude, than that of the bulk niobium cavity. This result agrees with what was found for 500 MHz cavities [10].

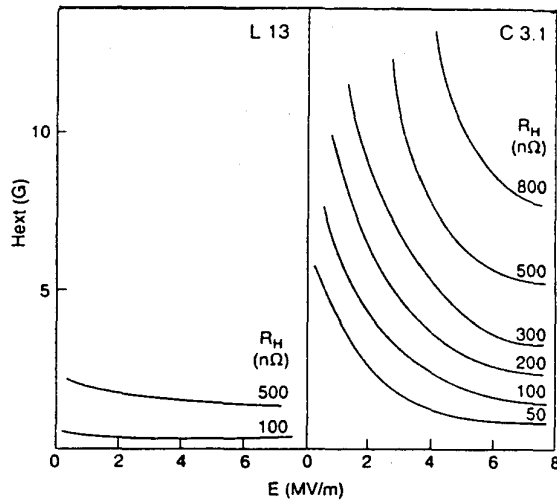


Figure 7.

3. Critical temperature

The average critical temperatures of the bulk niobium cavity and of two of the niobium copper cavities have been measured by observing the abrupt change in field

distributions when the cavity temperature increases beyond T_c [11]. The cavity under study was prepared in one of the two configurations (trapped state or Meissner state) described in the preceding section ($H_{ext} = 10$ G) and left to slowly warm up as small heat losses cause the cryostat temperature to increase at a typical rate of 0.7 K per hour. The cavity temperature was continuously monitored by a germanium thermometer at the equator and carbon thermometers on each of the cutoffs. The magnetic field distribution was measured, also continuously, with 9 Hall probes providing measurements of the magnetic field vectors at the equator and near each of the irises. Abrupt changes were observed when the temperature reached its critical value. Small differences between the times at which these changes occurred were found consistent with a simple model describing the evolution of the location of the transition plane along the cavity (taking into account the temperature gradient and time dependence). The uncertainties associated with this non uniformity of the temperature distribution across the cavity are included in the errors listed in Table 2.

The critical temperatures of the niobium copper cavities are observed to significantly exceed (by nearly 0.3 K) that of the bulk niobium cavity which is in a good agreement with values quoted in the literature [12]. This difference can be qualitatively assigned to the difference between the lattice parameters which characterize each of the two structures. The expected dependence of the critical temperature on the lattice expansion with respect to the bulk is shown in Figure 8 (from Reference [13]). A lattice expansion of 1.8 to $2.0 \cdot 10^{-3}$ nm has been measured at room temperature using X-ray spectroscopy, consistent with the combined effect of the presence of dissolved argon atoms and the different thermal expansion coefficients of niobium and copper between coating and room temperatures. When the temperature is lowered to ~ 10 K an additional thermal expansion effect of 0.2 to $1.0 \cdot 10^{-3}$ nm is expected to occur resulting in a prediction in the range of 9.5 to 9.8 K for the critical temperature [14].

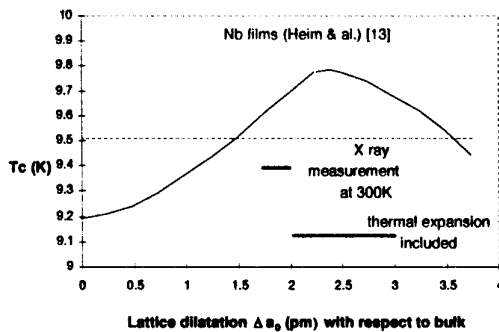


Figure 8.

	L13 (Nb)	B2.2 (Nb/Cu)	C3.1 (Nb/Cu)
T_c (K)	9.231	9.506	9.56
error (K)	0.032	0.016	0.03

Table 2.

Acknowledgements

The essential technical contribution of C. Dalmas, J. Bendotti and F. Grabowski is gratefully acknowledged. We thank R. Russo for illuminating discussions in relation with the T_c measurement. We are deeply indebted to J. M. Rieubland and his cryogenic group for their invaluable assistance and for providing excellent working conditions. We thank C. Benvenuti and his group and J. Tückmantel for their interest in our work and for useful discussions.

References

- [1] G. Cavallari et al., Proc. XVth Inter. Conf. High Energy Accelerators, Hamburg Germany July 20 - 24, 1992, ed J. Rossbach, Singapore (1993) 694.
- [2] E. Chiaveri et al., this conference.
- [3] C. Benvenuti et al., Appl. Phys. Lett. 45 (1984) 583.
- [4] Ph. Bernard et al., Proc. 5th workshop RF Supercond., ed. D. Proch, 19 - 23 Aug 1991, DESY, Hamburg, Germany, 487.
- [5] G. Cavallari et al., Proc. 4th EPAC London, 27 June - 1 July 1994, ed. V. Suller, Ch. Petit - Jean - Genaz, Singapore (1994), 2042.
- [6] J. M. Pierce, Methods of Experimental Physics, Vol. 11, Part 10, ed. Marton, Academic Press, New York (1994).
- [7] K. Halbach and RF. Holsinger, Part. Accelerators 7 (1976) 213.
- [8] T. Weiland, DESY 82 - 015 and DESY 11 - 82 - 24.
- [9] C. Vallet et al., Proc. 3rd EPAC, Berlin, 24-28 March, 1992, ed. H. Henke, H. Homeyer and Ch. Petit - Jean - Genaz, Gif - sur - Yvette (1992) 1295.
- [10] G. Arnolds - Mayer & W. Weingarten, IEEE Trans. Magn. MAG-23 (1987) 1620.
- [11] G. Arnolds - Mayer & C. Chiaveri, Proc. 3rd workshop RF superc., Argonne, Ill, USA, 1987, ed K. W. Shepard, ANL PHY 88 - 1, Argonne (1988) 491.
- [12] V. Z. Kresin & S. A. Wolf, Fundamentals of Superconductivity, Plenum Press, New York and London.
- [13] G. Heim & E. Kay, J. of Applied Physics, vol 46, N°9 (1975) 4006.
- [14] R. Russo, private communication.